THE SLOPE IMAGING MULTI-POLARIZATION PHOTON-COUNTING LIDAR: DEVELOPMENT AND PERFORMANCE RESULTS

Philip Dabney[1], David Harding[1], James Abshire[1], Tim Huss[2], Gabriel Jodor[2], Roman Machan[2], Joe Marzouk[2], Kurt Rush[1], Antonios Seas[1], Christopher Shuman[3], Xiaoli Sun[1], Susan Valett[1], Aleksey Vasilyev[4], Anthony Yu[1], and Yunhui Zheng[2]

[1]NASA Goddard Space Flight Center, Greenbelt, MD 20771, [2]Sigma Space Corporation, Lanham, MD 20706, [3]University of Maryland Baltimore County GEST, Baltimore, MD 21228, [4]Science Systems and Applications, Inc., Lanham, MD 20706

Abstract - The Slope Imaging Multi-polarization Photon-counting Lidar is an airborne instrument developed to demonstrate laser altimetry measurement methods that will enable more efficient observations of topography and surface properties from space. The instrument was developed through the NASA Earth Science Technology Office Instrument Incubator Program with a focus on cryosphere remote sensing. The SIMPL transmitter is an 11 KHz, 1064 nm, plane-polarized micropulse laser transmitter that is frequency doubled to 532 nm and split into four push-broom beams. The receiver employs single-photon, polarimetric ranging at 532 and 1064 nm using Single Photon Counting Modules in order to achieve simultaneous sampling of surface elevation, slope, roughness and depolarizing scattering properties, the latter used to differentiate surface types. Data acquired over ice-covered Lake Erie in February, 2009 are documenting SIMPL's measurement performance and capabilities, demonstrating differentiation of open water and several ice cover types. ICESat-2 will employ several of the technologies advanced by SIMPL, including micropulse, single photon ranging in a multi-beam, push-broom configuration operating at 532 nm.

I. INTRODUCTION

The Slope Imaging Multi-polarization Photon-counting Lidar (SIMPL) is an airborne laser altimeter developed through the NASA Earth Science Technology Office Instrument Incubator Program with a focus on cryosphere remote sensing. The SIMPL instrument incorporates beam splitting of a micropulse laser, single-photon ranging and polarimetry technologies at green (532 nm) and near-infrared (1064 nm, NIR) wavelengths in order to demonstrate measurement approaches of potential benefit for improved, more efficient spaceflight laser altimeter missions. The measurement configuration is a "push-broom" with four beams spaced apart perpendicular to the flight direction (Fig. 1). SIMPL's measurement capabilities provide information about surface elevation, roughness and slope as well as depolarizing scattering properties used to differentiate types of ice sheet and sea ice surfaces.

Prior work demonstrated micropulse, photon-counting laser altimetry at 532 nm using Photomultiplier Tube (PMT) detectors [1,2,3,4]. In addition, work using a non-ranging instrument documented that laser depolarization at 355, 532 and 1064 nm differentiates needle-leaf and broad-leaf vegetation and row crops based on differences in their wavelength-dependent scattering properties [5,6]. A subsequent modification to that instrument incorporating full waveform recording enabled polarimetric ranging at 532 and 1064 nm [7,8]. SIMPL integrates and advances these technologies in a 16-channel instrument having four beams each with two colors, with each color observed in directions parallel and perpendicular to the transmit polarization plane.

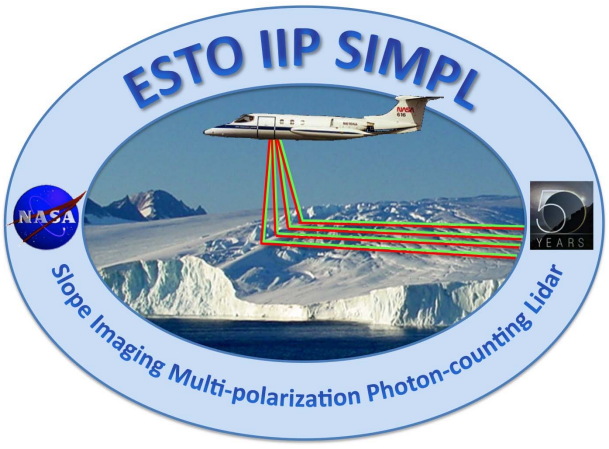

Figure 1. SIMPL beam geometry with four cross-track, 532 and 1064 nm beams forming four parallel, two-color profiles in the flight direction.

II. INSTRUMENTATION

A. Transmitter

SIMPL's laser transmitter and receiver optics are mounted on opposite sides of a thermally stable, 80 cm long optical bench and share the same 20 cm aperture off-axis parabola telescope in order to preserve alignment between the transmitter and receiver (Fig. 2). The Teem Photonics micropulse transmitter source is an 11.4 kHz pulse rate, 1064 nm microchip laser that emits ~8 mJ per pulse of linearly polarized light. The pulse width is slightly less than 1 nsec FWHM (Full Width Half Maximum). The NIR output is frequency doubled to 532 nm using a KTP nonlinear crystal. The dual wavelength beam is then spectrally separated using a dichroic beam splitter and each

color goes through its own transmit optical path. Each optical path separates the beams into four beams with parallel polarization planes. The two wavelength beam paths are then recombined using a second dichroic filter. Transmission through a lens array and reflection off the primary mirror toward the Earth's surface yields four 0.3 m laser footprints with each spaced cross-track by 8 m at the nominal flight altitude of 3.7 km.

B. Receiver

Laser energy reflected from the Earth's surface is collected by the primary mirror. A lens assembly focuses the received beams onto a 1 x 4 pinhole array. The pinholes define four small receiver fields of view (FOV), 0.9 m in diameter at the nominal flight altitude, that provide strong spatial filtering of solar background radiation.

The 532 and 1064 nm beams are separated by a dichroic plate and polarizing beam splitters further decompose the signals into those with polarization parallel and perpendicular to the transmit beams. The end result is four beam arrays that each have a particular wavelength and polarization state, yielding 16 signal channels. Each beam array passes through a mechanical iris used to control the effective receiver aperture and thus signal and solar background count rates.

The 16 signals are each optically fiber coupled to a spectral filter assembly to further reduce the solar background noise. Fiber optics are then used to transfer the filtered light to 16 PerkinElmer silicon avalanche photodiode Single Photon Counting Modules (SPCMs) housed in 4 quad assemblies [9]. SPCM's are used because they are the only mature, single photon, time-resolved detectors with sensitivity at both 532 nm (~65% quantum efficiency) and 1064 nm (~2% QE). A disadvantage of the SPCM's is that after detection of a photon they have a dead time of ~ 50 nsec (7.5 m) during which additional received photons cannot be detected. The dead time causes a range bias that is too short if additional signal photons per laser pulse are received within 50 nsec of the first detected photon. To minimize the bias the probability of detecting a signal photon is controlled, using the mechanical irises and by changes in flight altitude, to nominally be below 30%.

C. Electronics and Data System

Upon detection of a photon, the electrical pulse from an SPCM is transmitted to one of four custom electronics interface cards. Each card receives signals from a four-beam array, a signal for each laser fire time and a GPS once-per-second pulse. The combined events are transmitted to one of four FAST ComTec P7889 event timer cards that time tag each event with 100 psec resolution. The high precision timing and short laser pulse width achieve a single photon range precision of ~8 cm.

A sustained data rate up to 22 million time-tagged events per second recorded to RAID disk storage has been achieved by the data system. Photon detection events are not range gated; following a laser fire all detection events are recorded to a distance of 13 km. In this way, atmospheric profiling can be done to characterize cloud cover conditions through which the ranging measurements are made. Solar background noise counts dominate the detection events; typically only a few percent or less of the events are returns reflected from the surface. Post-flight processing software unpacks the data and sorts it by laser wavelength and polarization and computes the UTC event time and apparent time-of-flight for each detected photon.

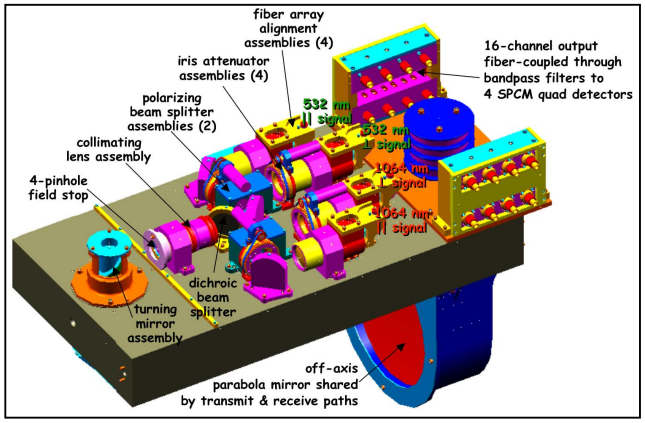

Figure 2. Mechanical schematic of the SIMPL optical bench, primary mirror and receiver-side components.

The SIMPL flights have been conducted on the NASA Lear-25 aircraft, operated by Glenn Research Center, that has a nadir viewing, optical port over which the optical bench is installed in a mounting frame. The additional SIMPL instrumentation is installed in two half-height 19-inch flight racks. Ancillary instrumentation consists of an Applanix Pos-AV system that provides orientation, position and time information and a nadir-viewing, digital video camera to document the flight line.

III. MEASUREMENT CHARACTERISTICS

The SIMPL data consists of "point cloud" profiles of single photon ranges that include spatially correlated surface returns and randomly distributed solar background noise. Aggregation of returns from a surface yields a range histogram (Fig. 3) that is a function of the transmit pulse shape, laser fire timing jitter, receiver bandwidth, surface "slope" (the incident angle between the laser beam and the surface normal), surface roughness at the laser footprint scale, and penetration into the surface, if transparent at the laser wavelength, resulting in volume scattering. The SIMPL transmit pulse shape consists of two components, a main asymmetric pulse and a broader, weaker after-pulse that occurs 8.3 nsec (1.25 m) after the main pulse. The instrument impulse response, accounting for the transmit pulse, timing jitter and receiver bandwidth, is 1 nsec FWHM, equivalent to 15 cm. Broadening of the range histogram beyond 1 nsec is due to the combined effects of surface slope, roughness and penetration.

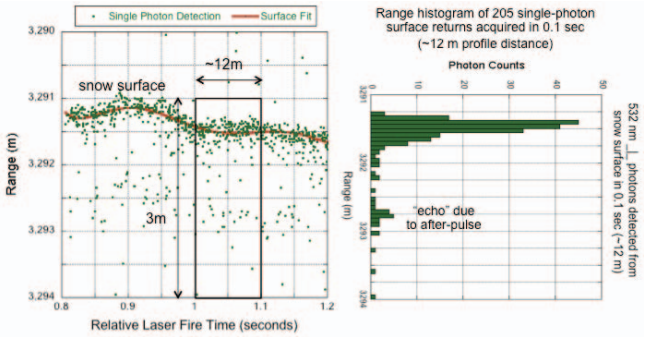

Figure 3. SIMPL single photon point cloud (for 532 nm perpendicular polarization) from a smooth, undulating snow surface (left) and an 18 cm FWHM range histogram (right) for 205 photons reflected from a flat segment acquired in 0.1 sec (~ 12 m).

The amplitude of the range histogram depends on the probability of detection (PD), the ratio of received photons reflected from the surface versus the number of transmitted pulses. The PD is a function of the surface retro-reflectance (at 0° phase angle with parallel illumination and view angles), ranging distance, atmospheric transmission and instrument parameters. At the 11.4 kHz pulse rate and nominal aircraft ground speed, flight altitude and iris aperture settings, single point measurements are typically acquired from ice surfaces every 3, 4, 6 and 9 cm for the 532 nm parallel (||) and perpendicular (_|_) channels and the 1064 nm || and _|_ channels, respectively.

III. ICE-COVERED LAKE ERIE RESULTS

SIMPL acquired data over Lake Erie on February 24 and 25, 2009 when ice cover was extensive. The ice cover, analogous to young sea ice, was a heterogeneous amalgam of fresh skim ice, thin dark nilas ice, grey ice and thicker grey-white ice. The lake ice is covered by snow in some places and broken by open water leads and irregularly shaped polynya. Measurement results are illustrated using a flight segment crossing dark nilas ice (A), grey-white ice (B and E), an open water lead (D), and a skim-ice covered polynya (C, Fig. 4, 5, 6). The character of the point cloud differs for the four channels illustrated by Beam 3 in Fig. 4. The PDs are indicated by the density of the surface return point cloud. Solar background noise is substantially larger at 532 nm due to higher solar irradiance and, for snow and ice surfaces, higher reflectance as compared to 1064 nm.

Fig. 5 shows the PDs for the same flight segment, computed for one-second increments. Amplitude differences between a channel's four beams are due to instrumental effects. Changes in PD are correlated with surface types having different reflectance and scattering properties. For single scatter events the reflecting photon's polarization plane remains parallel to that of the transmit pulse. In the case of specular reflection from a mirror-like surface or from water, consisting only of single scattering, all reflected energy retains a parallel polarization plane. This accounts for the lack of 1064 nm _|_ signal from open water (D). The

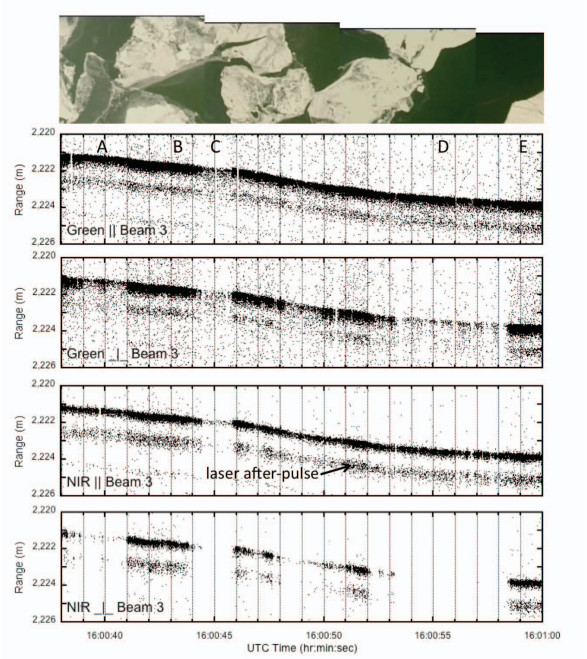

Figure 4. Point cloud profiles across Lake Erie ice cover for the four channels on Beam 3. The profile location is along the bottom edge of the video frame composite. Four surface types occur along the profile: dark nilas ice (A), grey-white ice (B, E), polynya covered by skim ice (C) and an open water lead (D). The profile length is ~ 260 m. The surface slope is due to uncompensated aircraft roll. The surface echo is due to the laser after-pulse. The vertical exaggeration is 43x.

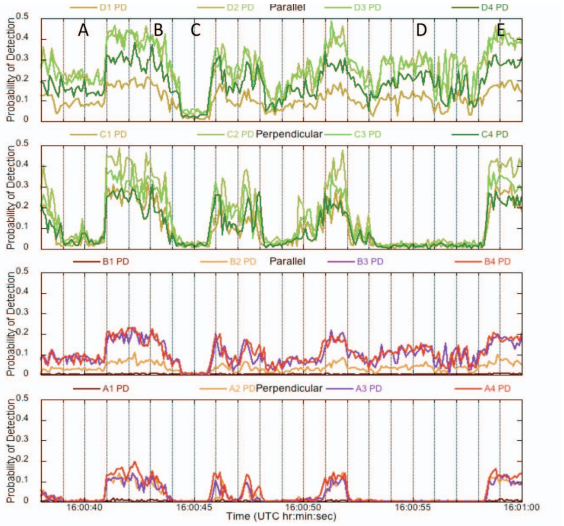

Figure 5. Probability of detection for each beam of the four channels. No 1064 nm || nor _|_ signal is detected for Beam 1 due to very low transmit energy and beam to pin-hole misalignment.

strength of the 532 and 1064 nm || signals specularly reflected back to the receiver depends on the fraction of the water surface that is oriented perpendicular to the incident beam, a function of wind speed.

During surface and volume multiple scattering the polarization plane of some reflected photons are rotated to be perpendicular to that of the incoming laser pulse. The

weak, open water 532 nm _|_ signal is due to volume scattering of green light that penetrated into the water column. An equivalent amount of 1064 nm light penetrates into the water column but it is all absorbed over a distance of a few cms. The grey-white ice (B, E) yields substantial signals in all four channels indicating that multiple scattering from a diffusely reflecting surface is occurring. The signal strengths of the nilas ice (A) are intermediate between that of the open water and the grey-white ice suggesting that a combination of specular, diffuse and volume scattering is occurring.

The polynya with skim ice cover (C) has no 1064 nm _|_ signal, very weak || signal and low 532 nm || and _|_ signals. It is inferred that the smooth skim ice is specular and, unlike the wind-roughened water surface, nearly all reflected || laser energy is directed at an angle away from the receiver because the laser beam is not normal to the surface. Micro-roughness is thought to be causing specular reflection of the very weak 1064 nm || signal back to the receiver. The 1064 nm _|_ signal is absent because all surface reflections are specular from the skim ice. The thin skim ice is transparent so green light is penetrating into the water column and undergoing volume scattering, accounting for the low 532 nm signals at both || and _|_ polarizations.

The changes in PD for the different surface conditions result in distinctive depolarization ratios, computed as the ratio _|_ PD / || PD (Fig. 6). A completely specular return has a depolarization ratio of 0. With increasing multiple scattering, the depolarization ratio increases. The ratios are normalized by the depolarization of a snow calibration surface, so that a surface with a value of 1 has depolarization equivalent to that of the snow target. Values greater than 1 are due to scattering causing depolarization greater than that of snow. The equivalent ratios, per wavelength, for each of the beams spaced cross-track by ~8 m indicates that they are traversing surfaces with the same scattering properties, except for a short segment occurring at 16:00:50. The open water (D) has very low and near-zero 532 and 1064 nm ratios, respectively (the non-zero 1064 nm result is due to _|_ background noise). The nilas ice (A) ratios are similar except for a higher 532 nm ratio corresponding to a lighter ridge observed in the video frame. The grey-white ice (B, E) has ratios comparable to that of the snow calibration target. The polyana skim ice has noisy ratios due to the very low 532 and 1064 nm || signals.

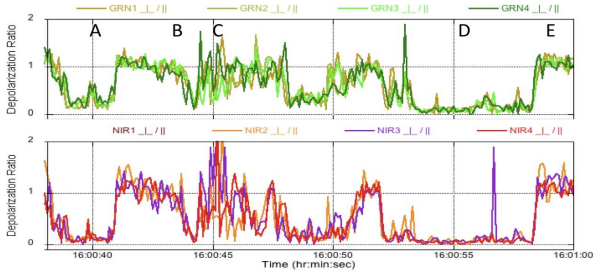

Figure 6. 532 and 1064 nm _|_ / || depolarization ratios for the four beams along the same flight segment depicted in Figs. 4 and 5. There is no 1064 nm ratio for Beam 1 due to the absence of _|_ and || signals.

IV. SIMPL AND THE ICESAT-2 MISSION

The experience gained developing SIMPL is benefiting formulation activities for the ICESat-2 mission [10]. ICESat-2, a follow-on to NASA's Ice, Cloud and land Elevation Satellite [11], is scheduled for launch in 2015. Like SIMPL, it will utilize a narrow pulse-width, high repetition rate, micropulse laser divided into multiple beams in a push-broom configuration. The receiver will time-tag single photon detections at 532 nm, using PMT array detectors, with 100 psec timing resolution electronics. At present there are no plans to simultaneously operate at 1064 nm nor acquire depolarization data.

SIMPL's data are being used to evaluate range biases due to 532 nm penetration into snow, ice and water, to assess variability in detection probability for these surfaces and to develop algorithms for on-board data acquisition and on-ground characterization of surface elevation, slope and roughness. In these ways, the development of the SIMPL instrument is meeting its objective of advancing technologies and methodologies in order to demonstrate measurement approaches of benefit for improved, more efficient spaceflight laser altimeter missions.

REFERENCES

[1] J.J. Degnan, J. McGarry, T. Zagwodzki, P. Dabney, J. Geiger, R. Chabot, C. Steggerda, J. Marzouk and A. Chu, "Design and performance of an airborne multikilohertz photon-counting, microlaser altimeter," *Proc. Land Surface Mapping and Characterization using Laser Altimetry, Int. Arch. Photogramm. Rem. Sens.*, vol. XXXIV3-W4, Annapolis, MD, pp. 9-16, 2001.

[2] J.J. Degnan, "Photon-counting multikilohertz microlaser altimeters for airborne and spaceborne topographic measurements," *J. Geodyn*., vol. 34(3-4), pp. 503-549, 2002.

[3] W.E. Carter, R.L. Shrestha and K.C. Slatton, "Photon counting airborne laser swath mapping (PC-ALSM)," in Gravity, Geoid and Space Missions, C. Jekeli, L. Bastos and J. Fernandes (Eds), Springer, IAG International Association of Geodesy Symposia, Vol. 129, pp. 214 - 217, 2004.

[4] T. Cossio, C. Slatton, W. Carter, K. Shrestha and D. Harding, "Predicting topographic and bathymetric measurement performance for low-SNR airborne lidar," *IEEE Trans. Geosci. Rem. Sens.*, vol. 47(7), pp. 2298 – 2315, 2009.

[5] J. E. Kalshoven, Jr., and P. W. Dabney, "Remote sensing of the Earth's surface using an airborne polarized laser," *IEEE Trans. Geosci. Remote Sensing*, vol. 31, pp. 438–446, 1993.

[6] J.E. Kalshoven, Jr., M.R. Tierney, Jr., C.S. T. Daughtry and J.E. McMurtrey III, "Remote sensing of crop parameters with a polarized, frequency-doubled Nd:YAG laser," *Appl. Opt.*, vol. 34, pp. 2745-2749, 1995.

[7] S. Tan, and R. Narayanan, "Design and performance of a multiwavelength airborne polarimetric lidar (MAPL) for vegetation remote sensing," *Appl. Opt.*, vol. 43(11), pp. 2360-2368, 2004.

[8] S. Tan, R.M. Narayanan, and S.K. Shetty, "Polarized Lidar Reflectance Measurements of Vegetation at Near-Infrared and Green Wavelengths," *Int. J. Infrared Millimeter Waves,* Vol. 26(8), pp. 1175-1194, 2005.

[9] X. Sun, et al., "Space-qualified silicon avalanche-photodiode single-photon-counting modules," *J. Modern Optics,* vol. 51(9), pp.1333-1350, 2004.

[10] W. Abdalati, et al., "The ICESat-2 Laser Altimetry Mission," *Proc. IEEE*, vol. 98(5), pp. 735-751, 2010.

[11] B.E. Schutz, H.J. Zwally, C.A. Shuman, D. Hancock, J.P. DiMarzio, "Overview of the ICESat Mission," *Geophys. Res. Lett.*, vol. 32: L21S01, doi:10.1029/2005GL024009, 2005.